A magnetically controlled tunable acoustic super-resolution lens

Peng Liu[1], Xing Chen[2], Zewei Hou[1] and Yongmao Pei[1(a)]

[1] *A State Key Laboratory for Turbulence and Complex Systems, Beijing Key Laboratory of Magnetoelectric Materials and Devices (BKL-MEMD), College of Engineering, Peking University - Beijing 100871, China*
[2] *A Energy Saving & Environmental Protection & Occupational Safety and Health Research Institute, China Academy of Railway Sciences Corporation Limited - Beijing 100871, China*

Abstract – Acoustic artificial structures have attracted much attention in recent decades due to their unique acoustic handling characteristics. The lightweight, easy-to-design feature and low cost of the thin-film acoustic artificial structure make it a great advantage in achieving super-resolution imaging and device miniaturization. However, since the film-type lens achieves super-resolution only at the resonance frequency, the frequency band in which it operates is greatly limited. In this work, considering the complexity of the vibration problem of the additional mass film, we propose a simple zero-mass method to design the operating frequency of the film-type prism. After that, a magnetic-field-controlled thin-film acoustic super-prism with a size of only six percent of the wavelength at working frequency is designed. Subsequently, based on the mechanism of magnetically induced stress, it achieves the super-resolution imaging within a frequency range from 350 Hz to 700 Hz. It provides a new idea for the design of an acoustic super-prism, and potential applications can be expected in acoustic imaging.

Introduction. – With the deepening of the research on the acoustic properties of composite materials and structures, it has been found that acoustic metamaterials have different properties from the materials of nature, and these structures are collectively referred to as acoustic artificial structures [1–3]. Acoustic artificial structures have attracted people's attention for their unique acoustic control characteristics in the past decade. The most attractive properties of acoustic metamaterials are band gap characteristics [4], defect state characteristics [5], negative refraction phenomena [6,7], acoustic hyperlens [8], acoustic rectifier [9,10], acoustic cloak [11–13], etc. Among them, super-resolution lenses of acoustic waves have important application prospects of the fields of medical ultrasonic testing and structural health monitoring, the limitations on resolution because the effects of diffraction have presented a significant barrier to generating and observing small features with acoustic waves. Many structures have been proposed to overcome this limit such as film material [8,14–18] and phased acoustic aperture [19–22].

Since super-resolution lenses utilizing the Fabry-Perot resonance require that the thickness of the structure must be an integer multiple of half a wavelength, this causes the structure to become larger. Therefore, due to its local resonance characteristics, thin-film acoustic metamaterials have attracted attention in achieving super-resolution imaging and device miniaturization. In 2011, Zhou *et al.* proposed a super-resolution lens model with anisotropic equivalent mass. When there is zero mass along the wave propagation direction, the evanescent wave can be amplified. It can be verified by numerical simulation that it can break through the diffraction limit [16]. Further, they constructed a super-resolution lens with a paper membrane and an aluminum waveguide [17]. In 2015, Gu *et al.* designed a trapezoidal film-type super-resolution lens. When zero mass is used, the phase velocity is close to infinity. In this way, the deflection of acoustic wave in ultrasonic wave is realized, and the resolution is improved [18]. As we mentioned before, the membrane-type super-resolution lens has a super-resolution function only near the resonance frequency. It is a problem that most resonant acoustic metamaterials have the disadvantage of narrow operating frequency bands.

(a)E-mail: pieym@pku.edu.cn

In this letter, we propose a simple design method for the equivalent zero-mass frequency of thin-film acoustic metamaterials. A super-resolution lens is designed based on this method. It achieves $\lambda/4.7$ super-resolution effects that break the diffraction limit. It has a dimension along the wave propagation direction that is only three percent of the wavelength of the resonant frequency. Then, based on the mechanism of magnetically induced stress [23–25], a low-frequency wide-band adjustable film-type super-resolution lens with a frequency adjustment range of 350 Hz is verified theoretically and experimentally.

Method. – The governing equation for thin-film metamaterials can be expressed as [23]

$$-\rho_1\omega^2\eta_1 - T\nabla^2\eta_1 = \Delta p,$$
$$-\pi R_2^2\omega^2\rho_2\eta_2 = \iint \Delta p\, dS_2 - F. \tag{1}$$

The first equation is the vibration equation of a circular elastic film under acoustic loading. The surface density of the elastic film is ρ_1, and the out-of-plane vibration displacement is η_1 under the action of the tension T. Because of the axial symmetry of the structure and the compressive load, the movement of the center mass can be described by the translational displacement η_2. Assuming that the areal density of the center mass is ρ_2, the film provides a restoring force F for the central mass. In the absence of load, the eigenvalue problem can be solved by solving the transcendental equation with the boundary condition that the outer diameter of the film is fixed, and the center mass and the film junction displacement are continuous. Consequently, the boundary conditions are expressed as

$$\eta_1(R_1) = 0,$$
$$\eta_1(R_2) = \eta_2(R_2). \tag{2}$$

Regardless of the non-axisymmetric modes, the general solution of the annulus membrane vibration is

$$\eta_1(r) = AJ_0(kr) + BY_0(kr), \tag{3}$$

where A and B are arbitrary constants; J_0 and Y_0 are Bessel functions of the first and second kind of order 0, respectively; k, defined as $2\pi f/c$, is the wave number in the annular membrane.

To more easily discuss the effect of structural parameters on the resonant frequency, we introduce a dimensionless parameter: $\alpha = R_2/R_1$, which represents the ratio of the center mass to the radius of the film, $\beta = \rho_2/\rho_1$, which represents the ratio of the center mass to the areal density of the film, and $\lambda = kR_1$, indicating a dimensionless wave vector. The relation between axisymmetric eigenfrequencies and the quantity can be calculated as: $f_i = c\lambda_i/2\pi R_1$, where $c = \sqrt{T/\rho_1}$ represents the wave velocity of the elastic membrane.

The eigenvalue equation is obtained:

$$Y_0(\lambda)J_0(\alpha\lambda) - J_0(\lambda)Y_0(\alpha\lambda) =$$
$$\frac{2}{\alpha\beta\lambda}[Y_0(\lambda)J_1(\alpha\lambda) - J_0(\lambda)Y_1(\alpha\lambda)]. \tag{4}$$
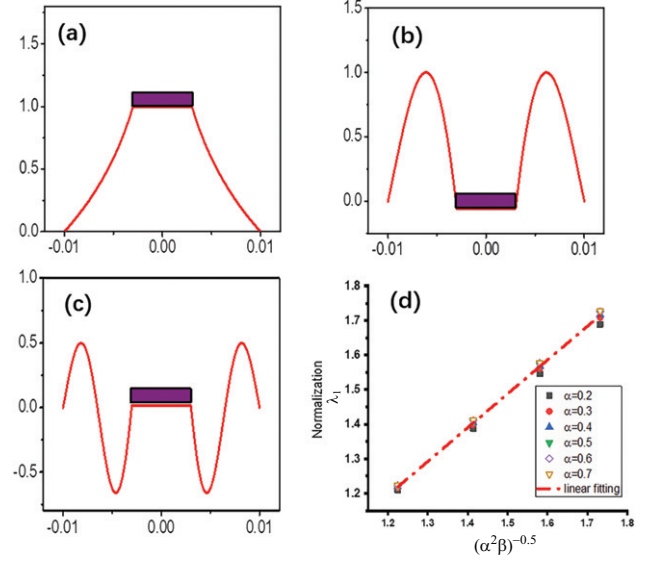

Fig. 1: (a) The first, (b) the second, (c) the third axisymmetric eigenmodes of the membrane-type acoustic metamaterial. (d) The relation of the first eigenfrequency and the mass with different radius ratio.

By numerically solving the eigenvalue equation, we can obtain a series of discrete eigenvectors corresponding to the resonant frequencies of each order. The first three order eigenmodes of thin-film acoustic metamaterials are shown in fig. 1.

It can be seen from eq. (4) that the dimensionless eigenvectors are only related to the parameters α and β. First, we study the effects of the parameters α and β on the first-order resonance frequency. We assume that the central iron piece is a concentrated mass and that the film acts like a spring, the square of the resonant frequency of the structure should decrease as the mass increase. After conversion to a dimensionless parameter, the mass of the center iron relative to the mass of the film can be expressed as $\alpha^2\beta$, and the first-order dimensionless quantity is expressed as λ_1. Under the premise of ensuring that the elastic film does not change, the first-order dimensionless eigenvector should satisfy the increase of the center mass: $\lambda_1\infty(\alpha^2\beta)^{-0.5}$. In order to verify the relationship, we calculate the theoretical solution of the central mass and the first-order dimensionless wave vector, as shown in fig. 1(d), in the case of different inner and outer diameter ratios. The dotted line is used as an auxiliary line to help determine whether there is a linear relationship. It can be seen that it is reasonable to simplify the first-order resonant state of the membrane structure, and the equivalent stiffness of the thin-film structure are determined only by the properties of the elastic film. Therefore, we consider that the first-order dimensionless eigenvectors λ_1 and α and β have the form as eq. (5a) below. As shown in fig. 1(d), the values of parameters A_1 and A_2 are determined to be 0.978 and 0.020, respectively, by parameter fitting.

Second, for the high-order resonance mode, it can be equivalent to the eigenvalue problem of the annular film
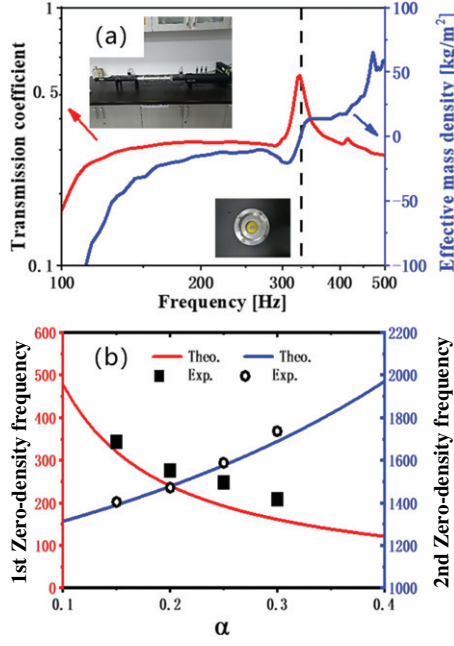
Fig. 2: (a) Transmission coefficients and equivalent mass density of super-resolved acoustic lens cells. The inset shows the unit cell and the experimental measurement device (Brüel & Kjær type-4206-T). (c) Experimental verification of the zero-mass frequency design formula.

with inner and outer simply supported boundary conditions, since the center mass is almost immobile, that is, the case where the right end of eq. (4) is zero. It is concluded that the higher-order eigenvectors with the center-attached mass film structure are independent of the surface density of the central mass. By approximating formula using the Bessel equation (5b), the eigenvalue equation of the ring membrane can be simplified to $\sin(\lambda - \alpha\lambda) = 0$. The solution to the high-order dimensionless eigenvector can be expressed as eq. (5c),

$$\lambda_1 = A_1(\alpha\sqrt{\beta})^{-1} + A_2, \tag{5a}$$

$$J_n \approx \sqrt{\frac{2}{\pi\lambda}} \cos\left(\lambda - \frac{n\pi}{2} - \frac{\pi}{4}\right),$$
$$Y_n \approx \sqrt{\frac{2}{\pi\lambda}} \sin\left(\lambda - \frac{n\pi}{2} - \frac{\pi}{4}\right), \tag{5b}$$

$$\lambda_i = \frac{(i-1)\pi}{1-\alpha}, \qquad i \geq 2. \tag{5c}$$

Results and discussion. – In order to verify the accuracy of the equivalent zero-mass frequency design formula, we design a corresponding verification experiment. The first-order zero-mass frequency is designed to be 350 Hz. An elastic film with a radius of 20 mm, a thickness of 0.075 mm and the estimated initial tension of 216 N/m is attached to the aluminum ring. The radius and thickness of the round iron in the center of the film are 3 mm and 1 mm, respectively. Using the acoustic impedance technique, the transmission coefficient of the cell and
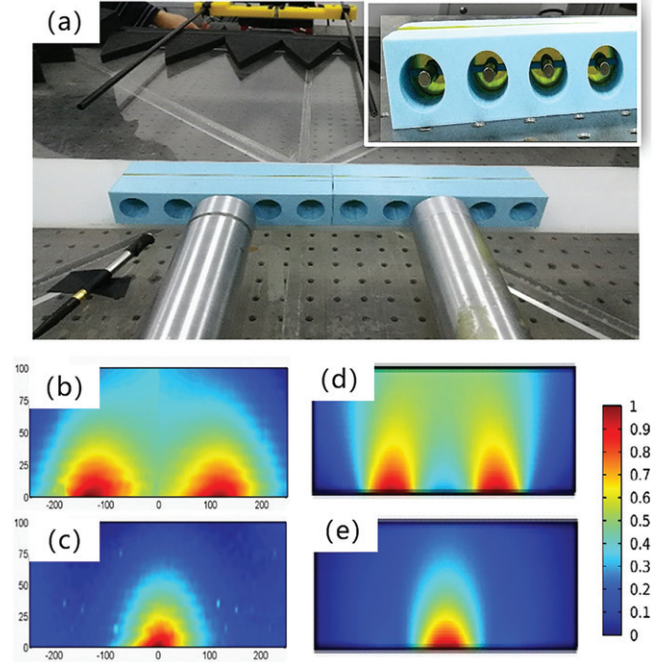

Fig. 3: (a) Two-dimensional sound field scanning experimental platform. The inset shows a 3D printed hyper-prism structure. (b) 350 Hz and (c) 400 Hz measurements of transmitted sound intensity distributions. (d), (e): distribution of the transmitted sound intensity in finite element simulations of 350 Hz and 400 Hz.
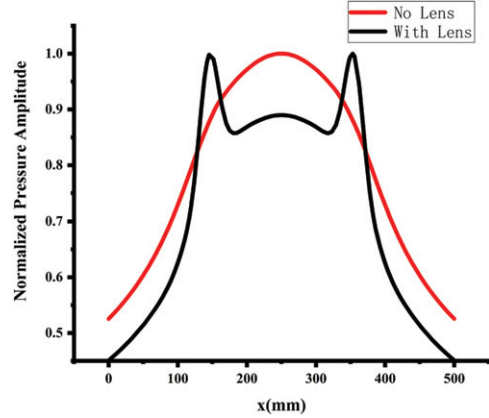

Fig. 4: Simulation results of the line distribution of normalized pressure amplitudes behind the lens, when two loudspeakers separated by 210 mm are placed in front of the lens.

the equivalent mass density of the film-type acoustic metamaterial can be measured, as shown in fig. 2(a). It can be seen that the experimentally measured structure has a resonant frequency of 328 Hz, corresponding to an equivalent zero mass, as indicated by the dashed line. In addition, the mass of the center rigid body can be changed by changing the number of irons. By changing the radius of the iron, the variation in the first two orders for zero-mass frequency is measured, as shown in fig. 2(b). The experimental results agree well with the theoretical design values. As the ratio of the radius increases, the stiffness
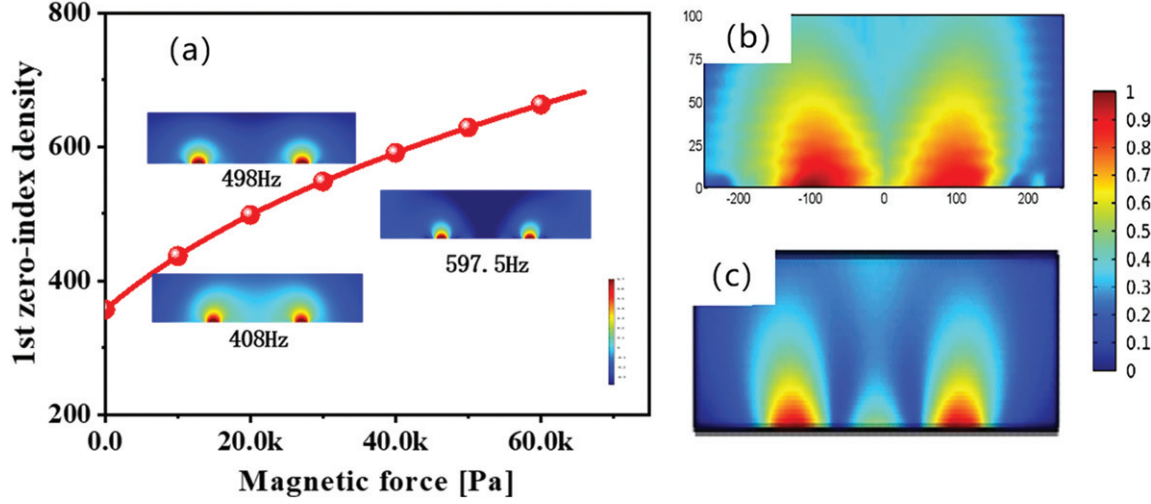
Fig. 5: (a) Magnetic force regulation range for zero-mass frequency. The inset shows the super-resolution effect of different frequencies under different magnetic controls. (b) 700 Hz measurements of transmitted sound intensity distributions. (c) Distribution of transmitted sound intensity in finite element simulations of 700 Hz.

of the center mass becomes larger, which makes the resonant frequency decrease. For the high-order resonance frequency, as the inner diameter of the ring film gradually increases, the rigidity of the structure increases, and the resonance frequency shifts upward.

As shown in fig. 3, we process a long strip structure with a circular cavity with a total length of 300 mm through the 3D printing technique. A clamp that holds the permanent magnet and fixed it in the super-resolution prism is designed. The magnetic force is controlled by adjusting the distance between the magnet and the center iron piece. Each hole in the fixture has a radius and depth of 10 mm, 30 mm, respectively, and a spacing of 30 mm between adjacent holes. The designed film-type metamaterial is pasted in the middle of the circular hole. The total thickness of the lens is about 60 mm. The two-dimensional acoustic field scanning platform is used to measure the transmitted sound field. The relevant sound pressure measuring devices we use are the microphone (Prestige MPA416) and the acquisition card (NI 9234). The acoustic lens is placed in the middle of a two-dimensional sound field having an area of $1000\,mm^2$ and surrounded by a sound absorbing material having a thickness of 150 mm. Two-point sound sources are arranged at the incident end, which is 2 mm away from the lens, and the distance between the two sound sources is 210 mm. We set up two microphones mounted on the electric table behind the lens, and the area that can be measured is $500 * 100\,mm^2$, which improves the efficiency of the experiment.

As shown in fig. 3(b) and fig. 3(d), when the frequency is close to zero-mass frequency (350 Hz), the presence of two point sources can be observed. It should be noted that due to the preparation of the film sample, the zero-mass frequency of the superlens is slightly different from the zero-mass frequency of the single-cell film. The diffraction limit

is broken due to a point source spacing of $\lambda/4.7$. When the frequency deviates from the zero-mass frequency (400 Hz), the existence of two-point sources cannot be resolved, as shown in fig. 3(c) and fig. 3(e).

To further illustrate the resolution of the lens, we extract the sound pressure distribution along the line in the finite element results for comparison. It is clear from fig. 4 that with the lens it is possible to distinguish the position of the two-point sources, whereas without the structure it is impossible to do so.

Further, when there is a magnetic field, the relationship between magnetic force and zero-mass frequency can be obtained by finite element simulation, as shown in fig. 5(a). The wide-band regulation effect of magnetic force on the first-order resonance frequency of the film has been explained in other works [23,25]. It is worth noting that the magnetic force can significantly change the stress state of the membrane, resulting in broadband effects. The greater the magnetic force, the greater the stiffness of the structure and the higher the resonant frequency. When the magnet slowly approaches the center of the iron piece, the attractive force caused by the magnetic field is estimated to be about 68 kPa. Not only 400 Hz can be distinguished, 700 Hz can still distinguish two sources, as shown in fig. 5(b). In addition, we use the commercial software package COMSOL Multiphysics to verify the zero-mass frequency in the design, enabling super-resolution imaging. By comparing the experimental results with the finite element results, it is further verified that the magnetic acoustic superlens can widen the operating frequency band.

Conclusion. – In summary, we propose a zero-mass design method for the membrane structure to simplify the solution of the membrane. Based on this method,

a super-resolution lens with a resolution of $\lambda/4.7$ is designed and verified by experiments. Furthermore, a continuous tunable acoustic lens is realized by using the design of magnetic stress enhancement of the thin-film structure. The problem of the narrowness of the film-type acoustic metamaterial is solved to some extent. The structure is light and simple, and is easy to prepare. It not only provides a feasible idea for the multifunctional design of acoustic devices but also offers the potential for wide applicability in extending beyond the traditional diffraction limits of acoustic imaging.

$$* * *$$

REFERENCES

[1] MA G. and SHENG P., *Sci. Adv.*, **2** (2016) 1501595.
[2] GE H., YANG M., MA C. *et al.*, *Natl. Sci. Rev.*, **5** (2018) 159.
[3] ASSOUR B., LIANG B., WU Y., LI Y., CHENG J.-C. and JING Y., *Nat. Rev. Mater.*, **3** (2018) 460.
[4] KUSHWAHA M. S. *et al.*, *Phys. Rev. Lett.*, **71** (1993) 2022.
[5] PSAROBAS I. E. *et al.*, *Phys. Rev. B*, **62** (2000) 5536.
[6] LI J., LIU Z. and QIU C., *Phys. Rev. B*, **73** (2006) 054302.
[7] FENG L. *et al.*, *Phys. Rev. Lett.*, **96** (2006) 014301.
[8] LI J. *et al.*, *Nat. Mater.*, **8** (2009) 931.
[9] LIANG B., GUO X. S., TU J., ZHANG D. and CHENG J. C., *Nat. Mater.*, **9** (2010) 989.
[10] DEVAUX T., TOURNAT V., RICHOUX O. *et al.*, *Phys. Rev. Lett.*, **115** (2015) 234301.
[11] ZHANG S., XIA C. and FANG N., *Phys. Rev. Lett.*, **106** (2011) 024301.
[12] POPA B.-I., ZIGONEANU L. and CUMMER S. A., *Phys. Rev. Lett.*, **106** (2011) 253901.
[13] ZIGONEANU L., POPA B.-I. and CUMMER S. A., *Nat. Mater.*, **13** (2014) 352.
[14] JIA H., KE M., HAO R. *et al.*, *Appl. Phys. Lett.*, **97** (2010) 173507.
[15] ZHU J., CHRISTENSEN J., JUNG J. *et al.*, *Nat. Phys.*, **7** (2011) 52.
[16] ZHOU X. and HU G., *Appl. Phys. Lett.*, **98** (2011) 263510.
[17] XU X., LI P., ZHOU X. and HU G., *EPL*, **109** (2015) 28001.
[18] GU Y., CHENG Y. and LIU X., *Appl. Phys. Lett.*, **107** (2015) 133503.
[19] GUILD MATTHEW D., ROGERS JEFFREY S., ROHDE CHARLES A. *et al.*, *Proc. SPIE*, **10600** (2018) 1060015.
[20] XIE Y., FU Y., JIA J. *et al.*, *Sci. Rep.*, **8** (2018) 16188.
[21] LI D., ZIGONEANU L., POPA B.-I. and CUMMER S. A., *J. Acoust. Soc. Am.*, **132** (2012) 2823.
[22] ZIGONEANU L., POPA B.-I. and CUMMER S. A., *Phys. Rev. B*, **84** (2011) 024305.
[23] CHEN X., XU X., AI S. *et al.*, *Appl. Phys. Lett.*, **105** (2014) 071913.
[24] CHEN Y., HUANG G., ZHOU X. *et al.*, *J. Acoust. Soc. Am.*, **136** (2014) 969.
[25] CHEN X., LIU P., HOU Z. and PEI Y., *Sci. Rep.*, **7** (2017) 9050.